

AD-A093 695

WISCONSIN UNIV-MADISON DEPT OF CHEMISTRY

F/G 7/4

LUMINESCENT PHOTOELECTROCHEMICAL CELLS. 4. ELECTROLUMINESCENT P-ETC(U)

DEC 80 H H STRECKERT, B R KARAS, D J MORANO

N00014-78-C-0633

NL

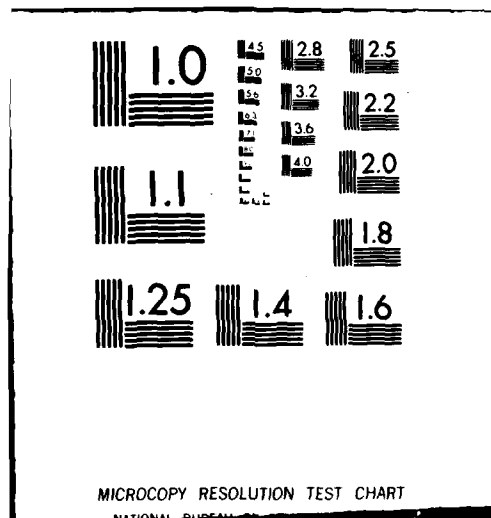
UNCLASSIFIED

TR-5

File 1  
400  
100-1001



END  
DATE  
FILMED  
2 -81  
DTIC



AD A093695

OFFICE OF NAVAL RESEARCH

Contract No. <sup>15</sup> N00014-78-C-0633

Task No. NR 051-690

<sup>9</sup> TECHNICAL REPORT NO. 5

<sup>12</sup>  
B.S.  
**LEVEL II**

<sup>6</sup>  
Luminescent Photoelectrochemical Cells. 4. Electroluminescent Properties of Undoped and Tellurium-Doped Cadmium Sulfide Electrodes

<sup>10</sup> by  
Holger H./Streckert, Bradley R./Karas, David J./Morano, Arthur B./Ellis

<sup>12</sup> <sup>27</sup>  
Prepared for publication

in the

Journal of Physical Chemistry

Department of Chemistry  
University of Wisconsin  
Madison, Wisconsin 53706

DTIC  
ELECTE  
JAN 13 1981  
S E

<sup>11</sup> 3 December 1980

Reproduction in whole or in part is permitted for any purpose of the United States Government

Approved for Public Release: Distribution Unlimited

\*To whom all correspondence should be addressed.

DOC FILE COPY

380155

81

1

12 053

Job

Unclassified

SECURITY CLASSIFICATION OF THIS PAGE (When Data Entered)

REPORT DOCUMENTATION PAGE		READ INSTRUCTIONS BEFORE COMPLETING FORM
1. REPORT NUMBER Technical Report No. 5	2. GOVT ACCESSION NO. AD-A093 695	3. RECIPIENT'S CATALOG NUMBER
4. TITLE (and Subtitle) Luminescent Photoelectrochemical Cells. 4. Electroluminescent Properties of Undoped and Tellurium-Doped Cadmium Sulfide Electrodes		5. TYPE OF REPORT & PERIOD COVERED
7. AUTHOR(s) Holger H. Streckert, Bradley R. Karas, David J. Morano, and Arthur B. Ellis		6. PERFORMING ORG. REPORT NUMBER
8. PERFORMING ORGANIZATION NAME AND ADDRESS Department of Chemistry University of Wisconsin Madison, Wisconsin 53706		9. CONTRACT OR GRANT NUMBER(s) (15) N00014-78-C-0633
11. CONTROLLING OFFICE NAME AND ADDRESS Office of Naval Research/Chemistry Program Arlington, VA 22217		10. PROGRAM ELEMENT, PROJECT, TASK AREA & WORK UNIT NUMBERS  NR 051-690
14. MONITORING AGENCY NAME & ADDRESS (if different from Controlling Office)		12. REPORT DATE December 3, 1980
		13. NUMBER OF PAGES 26
		15. SECURITY CLASS. (of this report) Unclassified
		15a. DECLASSIFICATION/DOWNGRADING SCHEDULE
16. DISTRIBUTION STATEMENT (of this Report)		
17. DISTRIBUTION STATEMENT (of the abstract entered in Block 20, if different from Report)  Approved for Public Release; Distribution Unlimited.		
18. SUPPLEMENTARY NOTES  Prepared for publication in the Journal of Physical Chemistry.		
19. KEY WORDS (Continue on reverse side if necessary and identify by block number)  electroluminescence; cadmium sulfide electrodes		
20. ABSTRACT (Continue on reverse side if necessary and identify by block number) Single-crystal, n-type, undoped CdS and Te-doped CdS (100, 1000 ppm CdS:Te) electrodes exhibit electroluminescence (EL) in aqueous, alkaline peroxydisulfate electrolyte. Addition of Te to CdS introduces intraband gap states which drastically alter the EL spectral distribution. The EL spectrum of undoped CdS consists of a sharp band near the band gap energy ( $\sim 2.4$ eV) with $\lambda_{\text{max}} \sim 510$ nm and a weaker, broader band at lower energy; the EL spectra		

DD FORM 1 JAN 73 1473

EDITION OF 1 NOV 65 IS OBSOLETE  
S/N 0102-LP-014-6601



Unclassified

SECURITY CLASSIFICATION OF THIS PAGE (When Data Entered)

Unclassified

SECURITY CLASSIFICATION OF THIS PAGE (When Data Entered)

of 100 and 1000 ppm CdS:Te also exhibit a sharp band at  $\sim 510$  nm but are dominated by broad bands with uncorrected  $\lambda_{\text{max}}$   $\sim 600$  and  $\sim 620$  nm, respectively. Photoluminescence (PL) spectra, obtained with 457.9 nm excitation, aid in the assignments of the emissive transitions; PL spectra are generally similar to their EL counterparts. The potential dependence of the EL spectra was examined between  $\sim -1.2$  V (onset) and  $-2.0$  V vs. SCE. Changes in potential can affect both the relative and absolute intensities of the bands present in the EL spectra. Lower limit, order-of-magnitude estimates of instantaneous EL efficiency,  $\phi_{\text{EL}}$ , have been made. Under steady-state conditions  $\phi_{\text{EL}}$  is  $\geq 10^{-6}$  for undoped CdS and  $\geq 10^{-5}$  for CdS:Te. Results are discussed in terms of interfacial charge-transfer processes and the excited-state manifolds of CdS and CdS:Te.

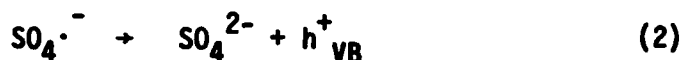
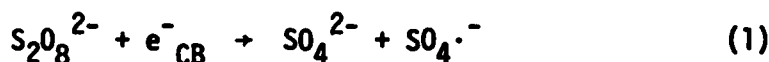
Accession For	
NTIS GRA&I	<input checked="checked" type="checkbox"/>
DTIC TAB	<input type="checkbox"/>
Unannounced	<input type="checkbox"/>
Justification	
By	
Distribution/	
Availability Codes	
Dist	Avail and/or Special
	

Unclassified

SECURITY CLASSIFICATION OF THIS PAGE (When Data Entered)

➤ An understanding of electrochemistry at semiconductor electrodes requires knowledge of the role intraband gap states play in mediating interfacial charge transfer. Reference to surface states is especially prevalent in the photo-electrochemical cell (PEC) literature.<sup>1</sup> The existence of intraband gap states has been supported in part by electroluminescence (EL) studies: Electrolyte species capable of hole injection into the valence bands of n-type, semiconducting  $\text{TiO}_2$ ,  $\text{SrTiO}_3$ ,  $\text{CdS}$ ,  $\text{GaP}$ ,  $\text{ZnO}$ , and  $\text{GaAs}$  yielded luminescence at sub-band gap energies.

Since the valence band edges of these materials are generally at very positive potentials, valence band hole injection requires a potent oxidizing species. Aqueous alkaline peroxydisulfate ( $\text{OH}^-$ ) $\text{S}_2\text{O}_8^{2-}$  electrolyte has been the medium of choice for observing the effect of the sequence of half-reactions occurring at the n-type semiconductor electrode is reported to be the following:<sup>4</sup>



The symbol  $e^-_{\text{CB}}$  represents an electron in or near (surface state or trap, e.g.) the conduction band; similarly,  $h^+_{\text{VB}}$  denotes a hole in or near the valence band. Once  $h^+$  has been injected by the strongly oxidizing sulfate radical, radiative recombination with electrons can occur. Estimates for the redox potentials of (1) and (2) are  $\leq +0.6$  and  $\geq +3.4$  V vs. NHE, respectively.<sup>5a</sup>

Establishing the presence of intraband gap states by EL-induced, sub-band gap emission demonstrates the utility of the technique. Extending EL studies beyond this stage would be greatly facilitated by knowledge of the energetic location and properties of the intraband gap states. Recent work in our laboratory has focussed on PECs employing n-type, Te-doped  $\text{CdS}$  ( $\text{CdS}:\text{Te}$ ) electrodes.<sup>7-10</sup> These materials exhibit room temperature photoluminescence (PL) at sub-band gap energies. The emissive transition involves well-characterized states introduced by the substitution of Te for S in the CdS lattice.

In this paper we demonstrate that the deliberate introduction of intraband gap states by Te lattice substitution significantly alters the EL properties of a CdS semiconductor electrode. Sections below detail the spectral distribution, voltage dependence and quantum efficiency of EL for undoped CdS, 100 and 1000 ppm CdS:Te. Comparisons with PL properties are discussed in terms of excited-state and interfacial charge-transfer processes.

### Experimental

**Materials** Single-crystal samples of n-type CdS, 100 ppm CdS:Te, and 1000 ppm CdS:Te were obtained from Cleveland Crystals, Inc., Cleveland, Ohio as 10x10x1 mm plates with the 10x10 face oriented perpendicular to the  $c$ -axis. These materials were vapor grown with resistivities (four point probe method) of  $\sim 2\Omega\text{-cm}$ . Values of [Te] are estimates based on starting quantities.  $\text{K}_2\text{S}_2\text{O}_8$  (Baker, 99.4%) was used as received.

**Electrode Preparation** Crystals were cut into irregularly-shaped pieces,  $\sim 0.3\text{ cm}^2 \times 1\text{ mm}$  and etched in a 1:10 (v/v)  $\text{Br}_2/\text{MeOH}$  solution for  $\sim 20\text{ s}$ . Samples were subsequently rinsed in distilled  $\text{H}_2\text{O}$ , transferred to a beaker of MeOH, and placed in an ultrasonic cleaner for 10 min. to remove residual  $\text{Br}_2$ . This etchant permits visual identification of the more specular 0001 "Cd"-rich and matte 000 $\bar{1}$  "S"-rich faces. Ohmic contact was made by rubbing Ga-In eutectic either on the 000 $\bar{1}$  face (leaving the 0001 face exposed) or on an edge ("edge mount"). A Cu wire was inserted into a 5 mm o.d. glass tube and attached to the eutectic by conducting Ag epoxy. Clear epoxy resin, used to protect the contact region from the electrolyte, was applied and, after curing, covered with black epoxy to eliminate emission from the mounting materials.

**Cells** All experiments were performed in a  $\text{N}_2$ -purged, 5M NaOH/0.1 M  $\text{K}_2\text{S}_2\text{O}_8$  aqueous electrolyte with a 1x3 cm Pt foil counterelectrode and an SCE. Electroluminescence (EL) and photoluminescence (PL) spectral measurements employed a 7.0x2.5 cm o.d. glass vessel. EL efficiency was measured using a "half-cell" described earlier.<sup>8</sup>

Current-Voltage Curves A standard three-electrode cell was used in conjunction with a PAR 173 potentiostat/galvanostat and a PAR 175 universal programmer which permitted the electrode potential to be swept or pulsed between preset values. The i-V curves were displayed on a Houston Model 2000 x-y recorder.

EL and PL Spectra Emission measurements (200-800 nm) were made on an Aminco-Bowman spectrophotofluorometer equipped with a Hamamatsu R446S PMT for extended red response. Uncorrected emission spectra were displayed on a HP7004A x-y recorder (response time,  $\sim 0.3$  sec); band width is  $\sim 5$  nm. EL spectra were obtained by pulsing the working electrode (CdS, CdS:Te) between 0.0 V (11 s) and -1.8 V vs. SCE (1 s) while the emission monochromator was scanned at 12 nm/min. This procedure was repeated for different geometries of the working electrode relative to the detection optics and for different electrode potentials in fixed geometries. In the latter case the more cathodic potential used in the pulse sequence was varied from the onset of EL ( $\sim -1.2$  to  $-1.3$  V vs. SCE) to -2.0 V vs. SCE and back to the onset potential; the EL spectra obtained at different potentials in this manner were most reproducible with potentials  $\lambda -1.8$  V vs. SCE. It should be noted that true EL peak intensities are not obtained in the pulse experiments due to the slow response time of the detection system. PL spectra represent front surface emission and were obtained by orienting the sample at  $\sim 45^\circ$  to both the 457.9 nm line of a Coherent Radiation CR-12 Ar ion laser and the emission detection optics. The 2-3 mm dia. laser beam was passed through an Oriel Model 7240 grating monochromator to eliminate background plasma lines, 10X expanded, translated upward and into the side of the emission compartment by a periscope, and masked to fill the electrode surface. Laser intensity was monitored by using a quartz disk as a beam splitter in conjunction with a Scientech 362 power energy meter.

EL Efficiency. Emission intensity was measured with a Tektronix J16 radiometer equipped with a J6502 probe head (flat response  $\pm 7\%$ , 450-950 nm). The flat window of the "half-cell" permits the  $1 \text{ cm}^2$  sensor area of the probe head to be within  $\sim 1$  cm of the sole exposed face of the emitting electrode. For steady-state, instantaneous EL efficiency determinations, the electrode was



held at  $-1.8$  V vs. SCE. Emission intensity and current were simultaneously recorded on Heath Model EU-200-02 and Varian Model 9176 strip-chart recorders, respectively. Gas quantities evolved from a 100 ppm CdS:Te electrode and a Pt counterelectrode during an EL experiment were collected by displacing electrolyte from inverted 10 x 0.5 cm o.d tubes with ends above the electrodes flared to 1 cm o.d. The ratio of gases collected at the two electrodes was roughly the same irrespective of whether the semiconductor electrode was held at  $-1.8$  V or pulsed between 0.0 V (11 s) and  $-1.8$  V vs. SCE (1 s). To identify the gases the same procedure was used except that 0.6 cm o.d. tubes were fitted with stopcocks such that a collection compartment of  $\sim 1.0$  cm<sup>3</sup> was obtained. After the electrolyte had been displaced from the compartments, the stopcocks were closed and the gases subsequently analyzed on a Kratos MS 902-C mass spectrometer.

### Results and Discussion

When a sufficiently negative bias is applied to n-type CdS and CdS:Te electrodes in a N<sub>2</sub>-purged, peroxydisulfate electrolyte (5M OH<sup>-</sup>/0.1 M S<sub>2</sub>O<sub>8</sub><sup>2-</sup>), luminescence is visibly apparent in a darkened room. Undoped CdS exhibits blue-green emission, while 100 and 1000 ppm CdS:Te emit orange and orange-red light, respectively. By conducting the EL experiment in the compartment of an emission spectrometer, the spectral distribution of emitted light can be analyzed as a function of various EL parameters.

In Figure 1 we present  $i$ -V curves for the CdS electrodes in both OH<sup>-</sup> and OH<sup>-</sup>/S<sub>2</sub>O<sub>8</sub><sup>2-</sup> media. Besides demonstrating that the current for potentials  $\geq -1.8$  V vs. SCE is largely a result of peroxydisulfate addition, Figure 1 also indicates the general electrochemical similarity of the three CdS materials. The onset of detectable EL for these samples is  $\sim -1.2$  to  $-1.3$  V vs. SCE. This range is negative of the estimated flat-band potential for undoped CdS in aqueous, alkaline media.<sup>4,11,12</sup>

As reported earlier for undoped CdS, the EL signal is most reproducible in a pulsed potential experiment.<sup>4</sup> In constant potential experiments conducted at -1.8 V vs. SCE, we found that a strong EL signal for 100 ppm CdS:Te diminished by at least an order of magnitude during the initial seconds that the cell was in circuit. We attribute the quenching primarily to the presence of surface Cd, initially formed via eq. 3; this reaction has been studied with undoped CdS in neutral aqueous media.<sup>13a</sup>



A dark layer is occasionally visible on the electrodes in  $\text{OH}^-/\text{S}_2\text{O}_8^{2-}$  electrolyte after several seconds at -1.8 V; evidence that the layer contains Cd is its oxidative removal at  $\sim -1.1$  V.<sup>13b</sup> The strong EL signal is regenerated by returning to -1.8 V vs. SCE. Our experiments have thus been conducted in a pulse sequence between 0.0 V (11 sec) and -1.8 V (1 sec). A net decomposition of CdS could occur under these conditions, but we found minimal weight loss in prolonged EL experiments.<sup>13c</sup> We interpret this to mean that although Cd may initially form by eq. 3, its subsequent presence is probably due to reduction of surface or electrolyte Cd-containing species ( $\text{CdO}$ ,  $\text{Cd}(\text{OH})_2$ , e.g.). It should be kept in mind that the effect of surface species on the EL spectral distribution by, e.g., absorption or reflection of the emitted light is unknown. However, both the EL spectral distribution and intensity were sufficiently reproducible (the intensity was constant to within  $\pm 10\%$  over hundreds of pulses) to permit characterization of the system.

### Spectral Distribution

The EL spectra of the three CdS electrodes are shown in Figures 2a, 3a, and 4a. Undoped CdS (Figure 2a) exhibits a sharp peak with  $\lambda_{\text{max}} \sim 510$  nm (FWHM  $\sim 15$  nm), as well as a weaker, broader band extending from  $\sim 600$  to 800 nm, the limit of our measuring capability. The 510 nm peak corresponds to roughly the band gap energy of CdS ( $E_{\text{BG}} \sim 2.4$  eV<sup>14</sup>). We assign the transition to the radiative recombination of an electron and hole with approximately conduction band edge and valence band edge energies, respectively; emission bands in this energetic vicinity have previously been reported in PL studies of undoped CdS.<sup>15</sup> Assignment of the lower energy transition(s) is hampered by the unknown location of intraband gap states which are clearly implicated

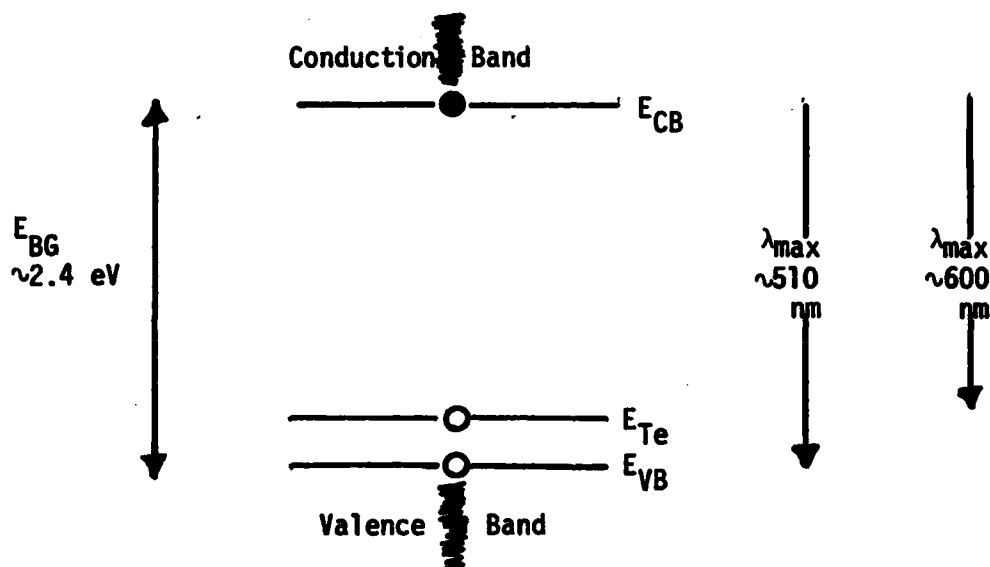
by the sub-band gap emission. This is the same problem which arose in the earlier study by Pettinger *et al.* on undoped CdS.<sup>4</sup>

For comparison with the EL spectrum, PL spectra of the same sample were obtained by exciting it with the 457.9 nm line of an Ar ion laser. Curves 1 and 2 of Figure 2b show the PL spectra of undoped CdS in air and peroxydisulfate electrolyte (open circuit to eliminate EL background), respectively. Because potential is known to influence photoluminescence<sup>7-10,16</sup>, we also examined the PL spectrum at -1.8 V vs. SCE in 5M OH<sup>-</sup> electrolyte where band bending should be more comparable to that of the EL experiment. In all of these PL spectra only the 510 nm band was detectable.

Although the uncertain origin of the low-energy EL band makes comparisons difficult, one possible explanation for its absence in the PL spectra may be relevant if surface states are involved in the emissive transition. Since the absorptivity of undoped CdS at 457.9 nm is  $\sim 10^5 \text{ cm}^{-1}$ ,<sup>14</sup> only a small fraction of light is absorbed at the surface. Any inefficiencies in populating the appropriate excited state with these photons would further reduce the probability for observing the low-energy emission band. On the other hand, the electrochemical generation of holes is a potentially more surface-sensitive technique: production of excited states is initiated at the semiconductor-electrolyte interface. Additionally, direct population of the emitting state is possible, depending upon the energy with which the hole is injected. Experiments designed to evaluate the surface sensitivity of EL are presently in progress.

Doping CdS with  $\sim 100$  ppm Te produces a dramatic change in the EL spectrum, Figure 3a. Although the sharp peak at 510 nm is still present, the EL spectrum is now dominated by a broad band with  $\lambda_{\text{max}} \sim 600$  nm. Both of these transitions are also observed in PL spectra in air and OH<sup>-</sup>/S<sub>2</sub>O<sub>8</sub><sup>2-</sup>, Figure 3b, and at -1.8 V vs. SCE in 5M OH<sup>-</sup> electrolyte. The origin of the 600 nm band is believed to be the introduction, by substitution of Te for S in the CdS lattice, of states  $\sim 0.2$  eV above the valence band edge.<sup>17-22</sup> Holes trapped at Te, which has a lower electron

affinity than S, can Coulombically bind an electron in or near the conduction band. This Te-bound exciton can radiatively collapse to produce the sub-band gap emission. A 100 ppm CdS:Te electrode thus has at least two excited states which can be populated in an EL experiment, as shown in a simplified one-electron diagram, Scheme I. The symbols  $E_{CB}$ ,  $E_{VB}$ ,  $E_{Te}$  and  $E_{BG}$  represent energies corresponding to the conduction band edge, the valence band edge, the Te states, and the band gap, respectively. Filled and open circles symbolize electrons and holes, respectively.

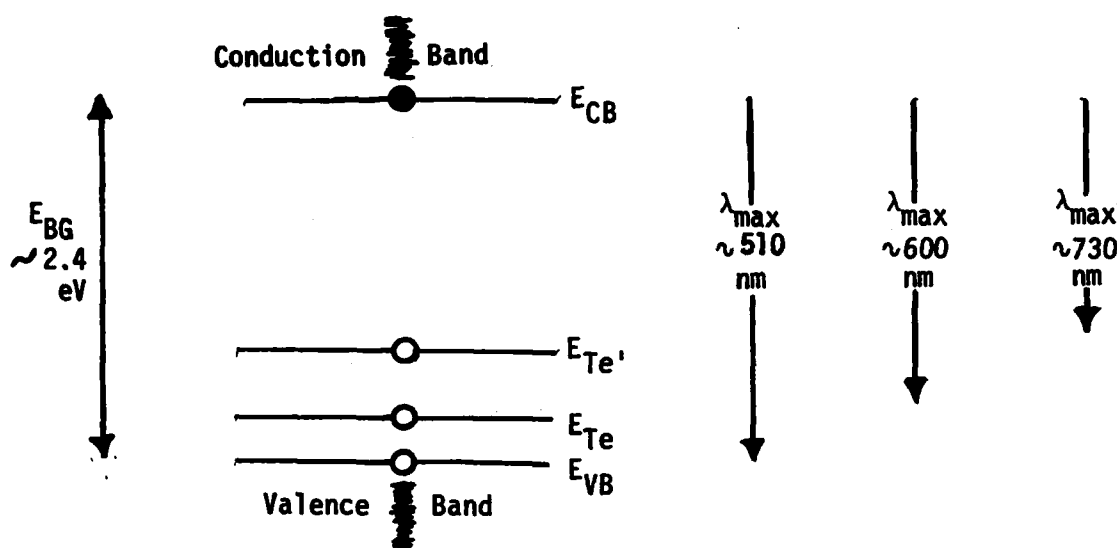


Scheme I

Introduction of Te into the CdS lattice is accompanied by the appearance of a low-energy absorption tail which masks the material's band gap.<sup>8,19-21</sup> While we cannot definitively assign the 510 nm transition in Figure 3, its energy, sharpness, and overall similarity to that of undoped CdS certainly suggest that it may be band edge-related. If so, this would confirm literature speculation that the CdS:Te band gap at low Te concentrations ( $[Te]$ ) is similar to that of undoped CdS.<sup>17b,19,21</sup> Edge emission for CdS:Te has been reported at low temperatures.<sup>19</sup>

One further comment regarding Figure 3a addresses the relative intensities of the 510 and 600 nm bands. Some of our samples gave visibly nonuniform EL properties. For these samples we found that the ratio of the 600 nm to the 510 nm intensity was dependent on the geometry of the electrode relative to the emission detection optics; for example, six different orientations of the sample used in the EL experiment of Figure 3a gave ratios of 4.5, 3.1, 2.9, 1.7, 1.5 and 1.3 (ratios are not corrected for a small amount of overlap of the 600 nm band tail with the 510 nm band). An analogous measurement in the PL experiment was precluded by the limited range of geometries which permitted both emission bands to be observed without interference from scattered laser light. The geometry-dependent EL spectra are likely a result of local variation in the electrode affecting some step(s) of the EL mechanism; excited-state decay kinetics should be especially sensitive to electrode nonuniformity. We emphasize that only some of our electrodes displayed geometry-dependent EL spectra.

It appears from both the PL and EL data for 100 ppm CdS:Te that Te states have a high probability of hole capture. This becomes even more evident in the 1000 ppm CdS:Te EL spectrum, Figure 4a. Although the sharp peak at  $\sim 510$  nm is still observable, its intensity is greatly diminished relative to a broad band with  $\lambda_{\text{max}} \sim 620$  nm. The 620 nm transition is likely a composite of bands: PL studies of  $\sim 1000$  ppm CdS:Te identified the 600 nm band observed for 100 ppm CdS:Te and a second band with  $\lambda_{\text{max}} \sim 730$  nm.<sup>18-21</sup> With increasing [Te] this latter transition becomes dominant in PL studies and is thought to arise from excitons trapped at several nearest-neighbor Te sites; the state involved ( $E_{\text{Te}_1}$ ) is believed to lie  $\sim 0.4$ - $0.6$  eV above the valence band edge.<sup>18-21</sup> A minimum of three excited states would thus exist for 1000 ppm CdS:Te, as sketched in Scheme II.



Scheme II

The PL spectra in air and peroxydisulfate electrolyte for the 1000 ppm CdS:Te sample are presented in Figure 4b. The emission maximum at  $\sim 640$  nm appears red shifted relative to the EL  $\lambda_{max}$  of  $\sim 620$  nm. This shift, well in excess of our band width of  $\sim 5$  nm, may not reflect differences in PL and EL so much as differences in potential. We find this shift duplicated in the PL spectra of 1000 ppm CdS:Te in 5M  $OH^-$  between  $-1.8$  V vs. SCE and open circuit; these spectra matched Figures 4a and b, respectively. In light of the above discussion, a plausible explanation for the spectral shift would be different efficiencies for hole capture by  $E_{Te}$  and  $E_{Te'}$  under the two sets of experimental conditions.

One disadvantage of the doped electrodes is that their emissive transitions mask the region where the low-energy band was observed in the EL spectrum of undoped CdS. There is no compelling reason to think that the states involved in that transition would be absent in the doped CdS samples. From the overall spectral envelope, however, we feel that the principal intraband gap states

contributing to the EL and PL spectra of CdS:Te are  $E_{Te}$  and  $E_{Te'}$ . We should point out that in no EL experiment did we see emission at  $200 \leq \lambda \lesssim 460$  nm.

#### Electrode Potential Effects

Previous studies indicated that the CdS EL intensity and spectral distribution were potential dependent.<sup>4a</sup> In Table I we present a summary of EL properties for the three CdS electrodes at potentials ranging from the onset of EL to -2.00 V vs. SCE. Table entries represent the maximum intensities observed at EL band maxima in the pulse-generated spectra (cf. Experimental); the insensitivity of the spectral distribution of individual EL bands to potential permits the data to be summarized in this form. In comparing tabulated intensities for a given electrode at several potentials, some caution in interpretation is necessary in the absence of time-resolved EL spectral data. Our preliminary time-resolved results indicate that peak EL intensity for these samples, occurring  $\sim 50$   $\mu$ sec after pulse initiation, does significantly increase with cathodic potential from -1.3 to -2.0 V vs. SCE in accord with the trends in Table I.

In several instances the relative intensities of the EL bands were also influenced by potential. Importantly, the spectral distribution found in the pulsed experiments was also observed, albeit at far lower intensities, in steady-state EL experiments conducted by sitting at the various potentials. To illustrate the potential dependence, the sample of undoped CdS examined (Part A, Table I) displayed a considerable increase in 510 nm emission relative to the 600-800 nm band in passing from -1.30 V to -1.55 V vs. SCE. Although little change was observed at -1.80 V, the intensity ratio of the two bands was again altered at -2.00 V vs. SCE, owing to the disappearance of the low-energy band. The efficiency of 510 nm emission relative to sub-band gap emission thus increased markedly on passing to more negative potentials.

Examination of 100 ppm CdS:Te (Part B, Table I) also revealed potential-dependent EL spectra. At the onset of EL,  $\sim -1.18$  V vs. SCE, only the 600 nm band was evident; even at -1.33 V this band dominated the 510 nm band as indicated by their intensity

ratio of 9. However, at -1.55, -1.80, and -2.00 V both bands contributed substantially to the emission with an intensity ratio ( $I_{600\text{ nm}}/I_{510\text{ nm}}$ ) ranging from  $\sim 3$ -5. For the 1000 ppm CdS:Te sample (Part C, Table I) the intensity ratio of the 620 nm to the 510 nm band was  $\sim 7$ -10 between -1.55 and -2.00 V vs. SCE. Interestingly, the 510 nm band was not detected at the most positive potential of -1.22 V vs. SCE, despite the very substantial 620 nm intensity.

This anomalously low 510 nm intensity is paralleled to a lesser extent by the -1.33 V experiment with 100 ppm CdS:Te and by what appears to be an EL onset at relatively more negative potential for undoped CdS. In other words, the 510 nm emission seems to require more negative potentials than the Te-based EL bands. In sharp contrast, 100 ppm CdS:Te does not exhibit potential-dependent intensity ratios in its PL spectra in 5M OH<sup>-</sup> electrolyte between -1.2 and -1.8 V vs. SCE. Determining whether the EL spectral dependence on potential is due to differences in population of the various excited states, differences in excited-state decay kinetics, differences in charge-transfer processes and rates, or a combination of these effects requires more mechanistic information than we presently possess. The result does accord, however, with previous studies<sup>4a</sup> in demonstrating that potential can provide selectivity over the EL spectral distribution in systems exhibiting multiple emission bands.

### Efficiency

Absolute determinations of EL efficiency are beset by several experimental difficulties; principally, these involve accounting for the spatial and spectral distributions of emitted photons and determining the fraction of current attributable to hole injection. Similar complications arise in measurements of electrogenerated chemiluminescence (ECL) efficiency.<sup>23</sup> We have adapted measures of efficiency from ECL studies which should yield lower-limit, order-of-magnitude values.<sup>23</sup> Our discussion will be confined to steady-state, instantaneous



EL efficiency,  $\phi_{EL}$ , as defined by eq. (4), where  $F$  is Faraday's constant. Data

$$\phi_{EL} = \frac{\text{Emitted Intensity (ein/sec)} \times F}{\text{Current Due to Hole Injection}} \quad (4)$$

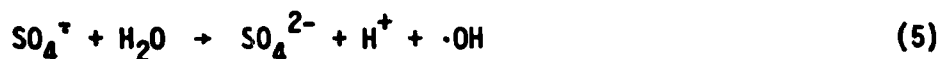
for this calculation are obtained from experiments conducted at constant potential.

We have attempted to measure the emitted light by placing a flat-response (450-950 nm) radiometer next to the sole, exposed face of the emitting electrode. The intensity in  $\mu\text{W}$  can be related to the photons emitted by the EL spectral distribution. Although all of our emission spectra are uncorrected, the similarity of our EL and PL spectral distributions suggest the use of corrected literature PL spectral data<sup>15b,20</sup> for this power to ein/sec conversion. The procedure is most straightforward and accurate for undoped CdS which has the majority of its EL intensity concentrated in the single, sharp band at  $\sim 510$  nm. The conversion is considerably less accurate for the doped electrodes which emit over a broad spectral range. Our estimate is made in this case by converting all of the power to photons at  $\lambda_{\text{max}}$  and bracketing this value by similar conversion to wavelengths near the extremes of the corrected spectra. In all cases we have underestimated the number of photons emitted, since not all of the photons are collected in the geometry employed.

Conversely, we have likely overestimated the denominator of (4) by using the total current as a measure of holes injected. If equations (1) and (2) truly describe the electrochemistry at the CdS electrodes, this procedure alone would cause us to underestimate  $\phi_{EL}$  by a factor of two. The factor could be even larger if allowance is made for reduction of  $\text{SO}_4^{2-}$  by conduction band electrons and for current due to the reduction of  $\text{H}_2\text{O}$ ,<sup>4a</sup> which Figure 1 suggests to be a competitive process. We estimate  $\text{H}_2\text{O}$  reduction to be a minor current contributor, however, based on collection of the gas evolved (analyzed by mass spectroscopy as largely  $\text{H}_2$ ) from a 100 ppm CdS:Te electrode: potentials of  $-1.8$  V vs. SCE (pulsed, as described earlier, or constant potential experiments) in

$\text{OH}^-/\text{S}_2\text{O}_8^{2-}$  electrolyte yielded  $\sim 1/8$  the gas volume collected at the Pt counter-electrode ( $\sim 1$  mol  $\text{O}_2$  was collected per 4 mol  $\text{e}^-$ ). For this set of conditions, then, electrolysis of  $\text{H}_2\text{O}$  accounts for only about 6% (1/16) of the current observed.

Our conservatism in using the total current in eq. (4) derives from consideration of nonelectrochemical means of generating hole-injecting radicals; in this case current is equated with holes injected. For example, thermal decomposition of  $\text{S}_2\text{O}_8^{2-}$  to  $2\text{SO}_4^\cdot$  is believed to occur<sup>24a</sup> and could, in fact, be catalyzed by the electrochemical conditions employed. Sulfate radicals produced in this manner can inject holes directly (eq. 2) or indirectly by eq. 5.<sup>24</sup>



The resulting  $\cdot\text{OH}$  radicals can then inject holes, as noted in the earlier CdS EL study.<sup>4a</sup>

With these considerations in mind, we made estimates of  $\phi_{\text{EL}}$  in constant potential experiments conducted at -1.8 V vs. SCE, Table II. We find that  $\phi_{\text{EL}}$  ranges from  $\sim 10^{-6}$  for undoped CdS to  $\sim 10^{-5}$  for 100 and 1000 ppm CdS:Te at current densities of  $\sim 5 \text{ mA/cm}^2$ . We suspect that EL efficiencies are considerably higher, particularly when the electrode is initially brought into circuit; for example, an EL efficiency of  $\sim 10^{-4}$  was previously reported under pulsed conditions for undoped CdS.<sup>4a</sup> A possible source of low EL efficiency under steady-state conditions is the presence of surface Cd (vide supra).

Although small in magnitude, the lower-limit estimates of  $\phi_{\text{EL}}$  do provide some insight into the EL mechanism. The expression for  $\phi_{\text{EL}}$  (eq. 4) can be further broken down into the product of an efficiency for excited-state population ( $\phi_{\text{ES}}$ , excited states populated per holes injected) and an emissive efficiency ( $\phi_{\text{r}}$ , photons emitted per excited states populated) which is characteristic of the excited state.<sup>23</sup> The general similarity in EL and PL spectral

distributions is good evidence that the same excited states are populated in both experiments. Estimates of  $\phi_r$  for the Te-based emission bands range from  $10^{-4}$ - $10^{-2}$  from PL studies.<sup>8,9,19,20</sup> If the same excited states and decay kinetics are involved in the EL and PL experiments, this  $\phi_r$  result in conjunction with the Table II entries suggests that  $\phi_{ES}$  for CdS:Te is no smaller than  $10^{-3}$  and is perhaps as large as  $10^{-1}$ . Improved estimates of efficiency require more detailed knowledge of both the interfacial charge-transfer processes and the nature of communication among the several excited states present in these systems. Studies designed to provide this information are in progress.

#### Acknowledgment

We are grateful to the Office of Naval Research for support of this work.

### References and Notes

1. See, for example, Bard, A.J.; Bocarsly, A.B.; Fan, F.F.; Walton, E.G.; Wrighton, M.S. J. Am. Chem. Soc. 1980, 102, 3671 and Wilson, R.H. J. Electrochem. Soc. 1980, 127, 228.
2. Noufi, R.N.; Kohl, P.A.; Frank, S.N.; Bard, A.J. J. Electrochem. Soc. 1978, 125, 246.
3. Mavroides, J.G. in "Semiconductor Liquid-Junction Solar Cells", Heller, A.; Ed., Proc. Vol. 77-3, Electrochemical Society, Inc., Princeton, N.J., 1977, p. 84.
4. (a) Pettinger, B.; Schöppel, H.-R.; Gerischer, H. Ber. Bunsenges. Phys. Chem. 1976, 80, 849. (b) Gerischer, H. J. Electrochem. Soc. 1978, 125, 218C.
5. (a) Memming, R. J. Electrochem. Soc. 1969, 116, 785. (b) Beckmann, K.H.; Memming, R. ibid. 1969, 116, 368. (c) Memming, R.; Schwandt, G. Electrochim. Acta. 1968, 13, 1299. (d) Memming, R.; Möllers, F. Ber. Bunsenges. Phys. Chem. 1972, 76, 609.
6. Benard, D.J.; Handler, P. Surf. Sci. 1973, 40, 141.
7. Ellis, A.B.; Karas, B.R. J. Am. Chem. Soc. 1979, 101, 236.
8. Karas, B.R.; Ellis, A.B. J. Am. Chem. Soc. 1980, 102, 968.
9. Ellis, A.B.; Karas, B.R. Adv. Chem. Ser. 1980, 184, 185.
10. Karas, B.R.; Morano, D.J.; Bilich, D.K.; Ellis, A.B. J. Electrochem. Soc., 1980, 127, 1144.
11. Ginley, D.S.; Butler, M.A. J. Electrochem. Soc. 1978, 125, 1968.
12. Inoue, T.; Watanabe, T.; Fujishima, A.; Honda, K. Bull. Chem. Soc. Jpn. 1979, 52, 1243.
13. (a) Kolb, D.M.; Gerischer, H. Electrochim. Acta 1973, 18, 987. (b) Both CdO and Cd(OH)<sub>2</sub> can form near this potential: Breiter, M.W. Electrochim. Acta 1977, 22, 1219 and references therein; (c) A 0.1292 g crystal of 100 ppm CdS:Te (~0.5 cm<sup>2</sup> surface area) lost ~0.2 mg of weight after 24 hr of continuous pulsing (1 sec each at 0.0 V and -1.8 V vs. SCE) in ~10 ml of OH<sup>-</sup>/S<sub>2</sub>O<sub>8</sub><sup>2-</sup> electrolyte. A quantity of Cd consistent with this weight loss was detected in the electrolyte by atomic absorption.

14. Dutton, D. Phys. Rev. 1958, 112, 785.
15. (a) Halsted, R.E. in "Physics and Chemistry of II-VI Compounds", Aven, M.; Prener, J.S., Eds. North Holland Publishing Co., Amsterdam, 1967, Ch. 8. Cf. Also Curie, D.; Prener, J.S. ibid., Ch. 9; Broser, I. ibid., Ch. 10; Morehead, F.F. ibid., Ch. 12. (b) Kulp, B.A.; Detweiler, R.M.; Anders, W.A. Phys. Rev. 1963, 131, 2036.
16. Petermann, G.; Tributsch, H.; Bogomolni, R. J. Chem. Phys. 1972, 57, 1026.
17. (a) Aten, A.C.; Haanstra, J.H. Phys. Lett. 1964, 11, 97. (b) Aten, A.C.; Haanstra, J.H.; deVries, H. Philips Res. Rept. 1965, 20, 395.
18. Cuthbert, J.D. J. Appl. Phys. 1971, 42, 739.
19. Cuthbert, J.D.; Thomas, D.G. J. Appl. Phys. 1968, 39, 1573.
20. Roessler, D.M. ibid. 1970, 41, 4589.
21. Moulton, P.F. Ph.D. Dissertation, Massachusetts Institute of Technology, 1975.
22. Bateman, J.E.; Ozsan, F.E.; Woods, J.; Cutter, J.R. J. Phys. D. Appl. Phys. 1974, 7, 1316.
23. (a) Faulkner, L.R.; Bard, A.J. in "Electroanalytical Chemistry", Vol. 10, Bard, A.J., Ed. Marcel Dekker, Inc., New York, 1977, pp. 1-95. (b) Keszthelyi, C.P.; Tokel-Takvoryan, N.E.; Bard, A.J. Anal. Chem. 1975, 47, 249. (c) Bard, A.J.; Keszthelyi, C.P.; Tachikawa, H.; Tokel, N.E. in "Chemiluminescence and Bioluminescence," Cormier, M.J.; Hercules, D.M.; Lee, J., Eds. Plenum Press, New York, 1973, pp. 193-208.
24. (a) Kolthoff, I.M.; Miller, I.K. J. Am. Chem. Soc. 1951, 73, 3055. (b) Tsao, M-S.; Wilmarth, W.K. J. Phys. Chem. 1959, 63, 346. (c) Heidt, L.J. J. Chem. Phys. 1942, 10, 297. (d) Dogliotti, L.; Hayon, E. J. Phys. Chem. 1967, 71, 2511.

Table I. Potential Dependence of Electroluminescence Spectra

A. Undoped CdS<sup>a</sup>

Potential, <sup>b</sup> V vs. SCE	Rel. Int. <sup>c</sup> 510 nm	Rel. Int. <sup>c</sup> 700 nm	I <sub>700 nm</sub> /I <sub>510 nm</sub> <sup>d</sup>
-1.30	38	4	0.1
-1.55	330	4	0.01
-1.80	390	4	0.01
-2.00	380	- <sup>e</sup>	- <sup>e</sup>

B. 100 ppm CdS:Te<sup>a</sup>

Potential, <sup>b</sup> V vs. SCE	Rel. Int. <sup>c</sup> 510 nm	Rel. Int. <sup>c</sup> 600 nm	I <sub>600 nm</sub> /I <sub>510 nm</sub> <sup>d</sup>
-1.18	- <sup>e</sup>	3	- <sup>e</sup>
-1.33	2 <sup>g</sup>	18	9 <sup>g</sup>
-1.55	79 <sup>g</sup>	398	5.1 <sup>g</sup>
-1.80	183 <sup>g</sup>	493	2.7 <sup>g</sup>
-2.00	320 <sup>g</sup>	1020	3.2 <sup>g</sup>

C. 1000 ppm CdS:Te<sup>a</sup>

Potential, <sup>b</sup> V vs. SCE	Rel. Int. <sup>c</sup> 510 nm	Rel. Int. <sup>c</sup> 620 nm	I <sub>620 nm</sub> /I <sub>510 nm</sub> <sup>d</sup>
-1.22	3 <sup>f</sup>	129	- <sup>f</sup>
-1.55	62 <sup>g</sup>	636	10.3 <sup>g</sup>
-1.80	210 <sup>g</sup>	1550	7.4 <sup>g</sup>
-2.00	80 <sup>g</sup>	810	10.1 <sup>g</sup>

a. The indicated n-type semiconductor was used as an electrode in a one-compartment EL experiment conducted in N<sub>2</sub>-purged, 5M NaOH/0.1M K<sub>2</sub>S<sub>2</sub>O<sub>8</sub> electrolyte; the Pt foil counterelectrode was 1 x 3 cm. Exposed electrode areas for undoped CdS, 100 ppm CdS:Te (edge-mounted) and 1000 ppm CdS:Te were 0.075, 0.71 and 0.41 cm<sup>2</sup>, respectively.

**Table I. continued**

- b. The semiconductor electrode was pulsed between 0.0 V vs. SCE (11 sec) and the indicated potential (1 sec) while the emission spectrum was scanned at 12 nm/min. A programmer-potentiostat was employed to cycle the electrode potential (cf. Experimental).
- c. Relative emission intensity at the indicated wavelengths which correspond to emission band maxima (700 nm was arbitrarily chosen for comparisons for undoped CdS). Since the geometry of each electrode relative to the emission detection optics was unchanged in passing from one potential to another, these values may be compared for a given electrode; it should be noted, however, that table entries are not true peak intensities and comparisons must be qualified by the absence of time-resolved data (see text and Experimental).
- d. Ratio of the relative emission intensities at the indicated wavelengths; this value is obtainable by dividing the values in the preceding columns. These are not absolute ratios because the emission spectra are uncorrected for detector response. The ratios are internally comparable for a given electrode, as described in footnote c, and were also obtained under steady-state conditions (see text).
- e. Band was not observed; consequently, ratios could not be calculated.
- f. This intensity appeared to be due entirely to the tail of the 620 nm band.
- g. No effort was made to subtract out intensity due to the tails of the 600 or 620 nm bands. The full intensity at 510 nm is entered in the table and used in the ratio calculations.

Table II. Estimates of Electroluminescence Efficiency

Electrode <sup>a</sup>	Emission Intensity, $\mu\text{W}(\text{ein}/\text{sec} \times 10^{12}; \lambda, \text{nm})^b$	$i, \text{mA}^c$	$\phi_{\text{EL}} \times 10^5^d$
Undoped CdS	0.0014(0.0060 ; 510)	1.1	0.53
100 ppm CdS:Te	0.014 (0.070 ; 600)	0.90	0.75
	(0.059 ; 500)		0.63
	(0.094 ; 800)		1.0
1000 ppm CdS:Te	0.064 (0.37 ; 700)	2.2	1.6
	(0.27 ; 500)		1.2
	(0.48 ; 900)		2.1

- The indicated n-type semiconductor was used as an electrode in a one-compartment EL experiment conducted in a  $\text{N}_2$ -purged  $5\text{M OH}^-/0.1\text{M S}_2\text{O}_8^{2-}$  electrolyte; the Pt foil counterelectrode was  $1 \times 3$  cm. Electrodes were held at  $-1.8$  V in these steady-state experiments. Exposed electrode areas were  $0.15$ ,  $0.29$  and  $0.41 \text{ cm}^2$  for undoped CdS, 100 ppm CdS:Te and 1000 ppm CdS:Te, respectively.
- Steady-state emission intensities measured in constant potential experiments with a flat-response radiometer. If all this power were concentrated at the single wavelength shown in parentheses, the indicated intensity in  $\text{ein}/\text{sec}$  is obtained. The first such wavelength for each electrode corresponds to an emission band maximum obtained from corrected literature PL spectra (see text). Subsequent values for the CdS:Te samples correspond to wavelengths near the extremes of the corrected emission spectra.
- Steady-state currents observed in constant potential experiments. For current densities divide by exposed electrode areas from footnote a.
- Instantaneous steady-state electroluminescence efficiencies calculated from the corresponding Table entries and eq. (4), using the total measured current in the denominator. From the approximations and assumptions used to obtain these data (see text), entries are best regarded as lower-limit, order-of-magnitude estimates.



## Figure Captions

**Figure 1.** Current-voltage curves for undoped CdS, 100 ppm CdS:Te, and 1000 ppm CdS:Te, labelled 1, 2, and 3, respectively. Dashed lines represent data obtained in 5M NaOH electrolyte; solid lines are plots obtained in 5M NaOH/0.1M  $K_2S_2O_8$  electrolyte. All curves were swept at 20 mV/sec. Electrode surface areas exposed to the electrolytes were 0.075, 0.71 and 0.41  $cm^2$  for undoped CdS, 100 ppm CdS:Te (edge mounted), and 1000 ppm CdS:Te, respectively.

**Figure 2 (a)** Uncorrected electroluminescence (EL) spectrum of undoped CdS obtained in 5M NaOH/0.1M  $K_2S_2O_8$  electrolyte. The electrode was continuously pulsed between 0.0 V (11 sec) and -1.8 V vs. SCE (1 sec) while the emission was scanned at 12 nm/min. Note the vertical scale expansion between 580 and 800 nm.

**(b)** Uncorrected photoluminescence (PL) spectrum of the same sample of undoped CdS in air (curve 1) and out of circuit but immersed in the peroxydisulfate electrolyte used for the EL experiment (curve 2). The sample was excited with the 457.9 nm line ( $\sim 5$  mW/ $cm^2$ ) of an Ar ion laser (excitation spike is shown at 1/100 the scale of the PL spectrum); scattered laser light accounts for the loss of baseline at the high-energy extreme of the PL spectrum. Sample geometry is identical in curves 1 and 2 but differs from that used in (a).

**Figure 3** Uncorrected EL (a) and PL (b) spectra of 100 ppm CdS:Te taken under the conditions given in Figure 2.

**Figure 4** Uncorrected EL (a) and PL (b) spectra of 1000 ppm CdS:Te taken under the conditions given in Figure 2.

